JOURNAL OF Materials CHEMISTRY

Nature of the strong electron donor 1,3,6,8-tetrakis(dimethylamino)pyrene and ionicity of its charge transfer complexes†

Gunzi Saito,*[a] Seiji Hirate,[a] Kazukuni Nishimura[a] and Hideki Yamochi[a,b]

[a]*Division of Chemistry, Graduate School of Science, Kyoto University, Sakyo-ku, Kyoto 606-8502, Japan. E-mail: saito@kuchem.kyoto-u.ac.jp*
[b]*CREST, Japan Science and Technology Corporation (JST),*

Received 11th September 2000, Accepted 8th December 2000
First published as an Advance Article on the web 7th February 2001

The 1,3,6,8-tetrakis(dimethylamino)pyrene (TDAP) molecule is a stronger electron donor (D) than conventional donor molecules such as tetramethyltetrathiafulvalene, *N*,*N*,*N*′,*N*′-tetramethyl-*p*-phenylenediamine and *N*,*N*-dimethyldihydrophenazine judged from both their charge transfer (CT) bands with *s*-trinitrobenzene (TNB) complexes and their redox potentials. The first averaged potential of oxidation and reduction peak potentials of TDAP is +0.02 V *vs.* SCE in acetonitrile. The molecule easily releases four electrons by two successive redox processes with two-electron transfer at each step as previously reported. Semiempirical calculation of molecular conformation infers that the peculiar redox behavior may be ascribed to the deformed conformations of cationic species of the TDAP molecule. Complex formation with a variety of acceptor molecules (A): TCNQs, *p*-benzoquinones and others was examined. With TCNQ derivatives, only tetrafluoro-TCNQ affords a 1 : 1 stoichiometry with an ionic ground state (D^{2+})(A^{2-}). The major ratio of the other CT complexes is 1 : 2, those with a strong acceptor in the TCNQ system have a completely ionic ground state; (D^{2+})(A^{-})$_2$ while those with a weak acceptor have a partial CT with the charge of TDAP between +1 and +2; $(D)^{+2(1-\delta)}(A^{-(1-\delta)})_2$ ($\delta \sim 0$). A very weak acceptor in the TCNQ system mainly affords the 1 : 3 complex with a partial CT state. In addition, the non-substituted TCNQ molecule affords a 1 : 4 complex with a partial CT state where the cationic species are deduced to be a mixture of $TDAP^{2+}$ and protonated TDAP. These partial CT compounds of TCNQs are highly conductive. The 1 : *n* (*n* = 2, 3, 4) complexes are found to contain anion species of $TCNQs^{-(1-\delta)}$ ($\delta \sim 0$) or a mixture of charge separated species ($A^{-\gamma} + A^{-(1-\delta)}$ or $A^{-(1-\delta)} + A^{-2(1-\gamma)}$: γ, $\delta \sim 0$). A very weak acceptor such as C_{60} or TNB affords a neutral complex. On the basis of the ionicity of TDAP CT complexes with TCNQs, *p*-benzoquinones and others, the criterion for partial CT is discussed.

1 Introduction

The fundamental requirement for high conductivity in molecular conductors is that the conducting component molecules satisfy both (a) partial charge transfer (CT) state in the electronic structure and (b) uniform segregated stack or layer in the solid structure.[1] When the system has uniform segregated stacks or layers and fulfils requirement (a), it becomes a metal except for the cases of a Mott insulator[2] and a charge localized system.[3] A few exotic exceptions have been noted; namely HMTTeF·Et_2TCNQ·THF_x,[4] C_{60} complexes[5] and 1 : 1 metallic complexes composed of extended π-systems.[6,7] The first exception violates requisite (b): it has an alternating DA stack and is metallic with a ground state composed of coexisting neutral and ionic species.

It is very rare in molecular metals for the degree of CT to be an integer, since it violates requisite (a). Among thousands of molecular metals so far prepared, only the anion radical salts of C_{60}[5] and the cation radical salts of tetrathiomethyl-TTP (tetrathiapentalene)[6] and tetrachalcogenoanthracene derivatives[7] are well-characterized metals with integer CT. Their metallic nature may stem from either the smaller effective on-site Coulomb repulsion U_{eff} than the bandwidth W for the latter cases or the degeneracy of the t_{1u} orbital of C_{60} that relaxes the Mott criterion.[8] However, for the A_nC_{60} case (A: alkali or alkaline earth metal), the occurrence of an integer of CT is, in fact, still controversial. The main chemicals which appear in this paper are shown in Fig. 1.

The complete transfer of an electron in the low-dimensional 1 : 1 DA CT complex is achieved in the appropriate combination of strong electron donor and acceptor molecules when the difference in their redox potentials ($\Delta E(DA) = E^1_{1/2}(D) - E^1_{1/2}(A)$) satisfies eqn. (1).

$$\Delta E(DA) < -0.02 \text{ (V } vs. \text{ SCE in } CH_3CN) \quad (1)$$

SCE is saturated calomel electrode and $E^1_{1/2}$(D) and $E^1_{1/2}$(A) are the first redox potentials of donor and acceptor molecules, respectively.[1b] Although the fully ionic complexes are commonly insulators or semiconductors, some of them have exhibited intriguing physical features such as a Mott insulating state,[9] antiferro- (or ferro-) magnetic interactions[10] or spin-Peierls state.[9,11]

So far a number of strong electron donor molecules with an aromatic planar molecular plane have been synthesized. However, suitable compounds with negative redox potentials (*vs.* SCE) as well as being stable as a neutral form at ambient conditions are limited[12] and their CT complexes have not been elucidated well.

1,3,6,8-Tetrakis(dimethylamino)pyrene (TDAP) has been reported by Ueda, Sakata and Misumi to have a negative $E^1_{1/2}$ value of −0.12 V *vs.* SCE in CH_3CN with two-electron

†Tables of crystallographic and structural refinement data, atomic positions, bond lengths and angles, anisotropic thermal parameters of TDAP and of elemental analysis, and a figure of the absorption spectrum of TDAP are available as supplementary data. For direct electronic access see http://www.rsc.org/suppdata/jm/b0/b007319i/

DOI: 10.1039/b007319i

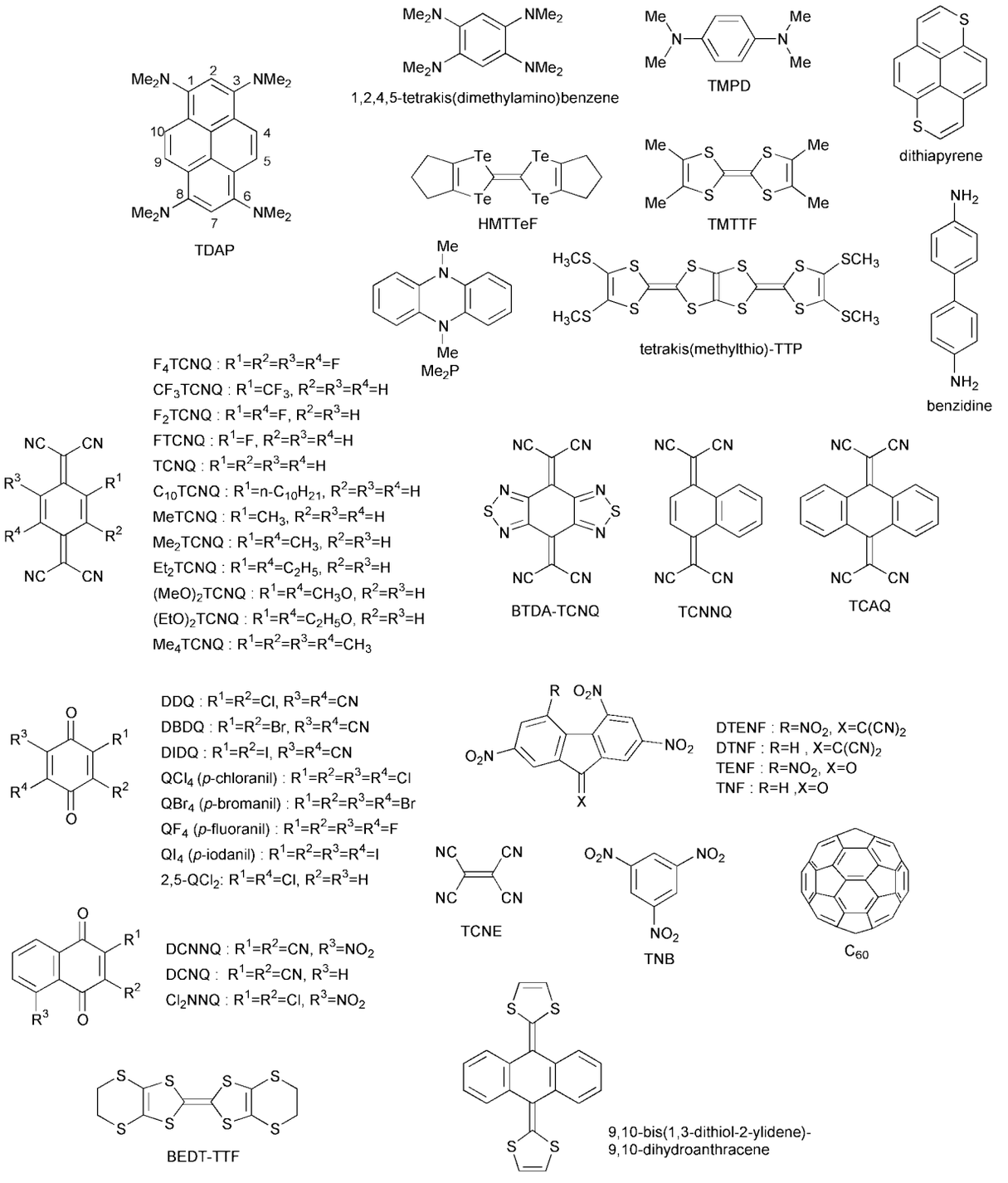

Fig. 1 Chemical structures of compounds discussed in the text.

transfer.[13] This implies that the on-site Coulomb repulsive energy of a TDAP molecule (bare U: U_0) is negligible and the monocation species of TDAP is difficult to isolate. Based on the redox potential of TDAP, it is also expected that the C_{60} molecules would provide either a neutral CT complex close to the neutral–ionic boundary or a partial CT state. This expectation stems from the requirement for the partial CT state for a 1 : 1 DA complex of the TTF·TCNQ system as shown in eqn. (2).[1b]

$$-0.02 \leq \Delta E(\mathrm{DA}) \leq 0.34 \text{ V} \qquad (2)$$

We report here the physical properties and structure of TDAP. CT complex formation of TDAP is also described in order to elucidate the electronic nature of TDAP in complexes and to establish the ionicity criterion of the TDAP CT complex.

2 Experimental

2.1 Synthesis

TDAP was prepared from 1,3,6,8-tetranitropyrene according to the method of Ueda, Sakata and Misumi.[13] The crude product (20.5 g) was purified twice by a conventional sublimation then once by a gradient sublimation to give 5.6 g of yellow prisms. Even though the mp, IR and UV spectra showed little difference from those of the reported ones[13] [mp 206.5–206.6 °C (dec.), lit. 212–213 °C; IR(KBr) 1597 cm^{-1}, lit. 1585 cm^{-1}; UV(CH_3CN) 228.0, 300.0, 419.0 nm, lit. 228, 302, 414 nm; elemental calc. for $C_{24}H_{30}N_4$: C, 76.97; H, 8.07;

N, 14.96; found C, 77.24; H, 8.07; N, 15.15%] and crystal structural analyses identified the material as TDAP.[14]

The tetrakis-hydrochloride salt of TDAP was prepared by treating TDAP with excess conc. HCl solution. The yellowish white precipitates were dried under vacuum (87% yield). The ratio of $(H_4TDAP^{4+})(Cl^-)_4(H_2O)_x$ ($x=1.5$–2) satisfies the elemental analysis result (calc. for $x=1.5$: C, 52.66, H, 6.81, N, 10.24, O, 4.38, Cl, 25.91; $x=2$: C, 51.81, H, 6.88, N, 10.07, O, 5.75, Cl, 25.49; found C, 53.06, 52.56, H.6.50, 6.50, N, 10.29, O, 4.81, Cl, 25.34%).[14]

The CT complexes were prepared either by direct mixing of the donor and acceptor dissolved separately in appropriate solvent or by the diffusion method. The complexes were obtained as powders except for the polycrystalline C_{60} complex. The single crystal growth of CT complexes for structural analysis by the diffusion method was not successful.

A comparison of the absorption spectra of neutral TDAP, $(TDAP)(I_3)_{2.1}$ and $TBA{\cdot}I_3$ in solid or solution clearly indicates that the bands at *ca.* 18×10^3 and 21–22×10^3 cm^{-1} are attributable to the $TDAP^{2+}$ species. The tetrakis-hydrochloride salt of TDAP ($TDAP:HCl:H_2O=1:4:1.5$–2) also exhibits three main bands (23.1, 31.7–34.1, 43.0×10^3 cm^{-1} in methanol *cf.* 21.8, 27.9–29.0, 36.0×10^3 cm^{-1} in solid). The absorption spectra are provided as supplementary data.†

2.2 Measurements

Melting points were not corrected. Cyclic voltammetry was performed in 0.1 M solutions of tetrabutylammonium tetrafluoroborate ($TBA{\cdot}BF_4$) in CH_3CN with Pt electrodes *vs.* SCE at a scan speed of 10–200 mV s^{-1} on a Yanaco Polarographic Analyzer P-1100 at 20–22 °C. Optical measurements were carried out with a KBr disk on a Perkin-Elmer Paragon 1000 spectrometer for IR and near-IR regions (400–7800 cm^{-1}) and on a Shimadzu UV-3100 spectrometer for near-infrared, visible and ultraviolet (UV–Vis–NIR) region (3800–42000 cm^{-1}). DC conductivities were measured based on a standard two- or four-probe technique attaching gold wires (15–25 μm diameter) to compressed pellet samples by gold paste (Tokuriki 8560-1A). EPR measurements were performed on a JEOL-TE200 X band EPR spectrometer with TE_{011} cavity whose temperature was varied from room temperature (RT) to 3 K by means of an Oxford ESR-910 cryostat. Static magnetic susceptibility was measured by the aid of SQUID magnetometer (Quantum Design MPMS) from 300 to 2 K. The stoichiometries of complexes were determined by elemental analysis (C, H, N, O, halogens) as provided in the supplementary table.†

The intensity data of the structural analysis were collected on an automatic four circle diffractometer or a oscillator type X-ray imaging plate with a monochromated Mo-Kα radiation at RT. The structures were solved by direct methods using SIR 92 program.[15] The refinements of structures were performed by full matrix least squares method (CRYSTAN 6.3). The parameters were refined adopting anisotropic temperature factors for non-hydrogen atoms of the donor molecules. The positions of hydrogen atoms were calculated by assuming a C–H bond of 0.96 Å and sp^3 conformation of the carbon atoms. The temperature factors of hydrogen atoms were fixed $U=0.050$. The atomic coordinates, equivalent isotropic thermal parameters, bond lengths and angles of TDAP are provided as a supplementary table.‡

The semiempirical molecular orbital calculations were performed using MOPAC 97 with the AM1 (RHF) parametrization.

‡CCDC reference number 1145/267. See http:///www.rsc.org/suppdata/jm/b0/b007319i/ for crystallographic files in .cif format.

3 Electron donating ability of TDAP

3.1 Redox potential

The cyclic voltammogram (CV) under our standard conditions (0.1 M $TBA{\cdot}BF_4$, CH_3CN, Pt, SCE) displayed two reversible redox waves with the peak separation of $\Delta E^1=26$–28 and $\Delta E^2=32$–38 mV for the first and second redox processes, respectively, below +0.50 V (Fig. 2 and Table 1). The CV data in different conditions are summarized in Table 1, where the averaged potential of the oxidation and reduction peak potential is defined as redox potential ($E^1_{1/2}$, $E^2_{1/2}$). The shape of the spectrum is the same as that reported in the literature.[13] However, the $E^1_{1/2}$ and $E^2_{1/2}$ values are not negative as reported previously (−0.12 and −0.05 V *vs.* SCE in CH_3CN)[13] but a little positive: +0.018 and +0.080 V at 100 mV s^{-1} or +0.006 and +0.080 V at 10 mV s^{-1}.

It is of interest to know what causes the difference between the observed and reported $E_{1/2}$ values. The main differences in the measuring conditions are the kinds of supporting electrolyte ($TBA{\cdot}BF_4$ *vs.* tetraethylammonium(TEA)·ClO_4) and the working electrode (Pt *vs.* glassy carbon). By using 0.1 M $TEA{\cdot}ClO_4$ as an electrolyte, the $E^1_{1/2}$ and $E^2_{1/2}$ values were 20–40 mV more negative. While the change of working electrode from Pt to glassy carbon resulted in a negative shift of the $E_{1/2}$ values by 20–50 mV. Using the combination of glassy carbon and 0.1 M $TEA{\cdot}ClO_4$, see ref. 13, we have observed the $E^1_{1/2}$ and $E^2_{1/2}$ values of −0.045 and +0.024 V, respectively, at a scan speed of 50 mV s^{-1}. The reason for the further negative shift by 0.07–0.08 V in ref. 13 is not clear at present.

The point of interest observed in Fig. 2 and Table 1 is the narrow peak separations ΔE^1 and ΔE^2 compared to the ideal peak separation of 59 mV for one-electron redox process. Such peak separations of 20–38 mV strongly suggest that each redox process involves two-electron transfer as pointed out by Ueda, Sakata and Misumi.[13] The redox potentials did not change within experimental errors by changing the sweep speed v from 10 to 200 mV s^{-1}, where a linear relation between peak current and $v^{1/2}$ is observed confirming that the process is diffusion limited.

Between +0.50 and +1.20 V two further redox processes were detected (Fig. 2), a quasi-reversible one at +0.71 V and irreversible one at +0.98 V with the peak separation of *ca.* 70 and 100 mV, respectively. The observation of the nearly ideal peak separation for the one-electron redox process at +0.71 V ensures that each redox process between 0.0 and +0.1 V certainly involves a two-electron transfer. Therefore it is evident that four electrons were released from TDAP in two steps with two electrons at each step in the narrow range of +0.0 to +0.1 V *vs.* SCE.

It is very remarkable that the difference of $E^1_{1/2}$ and $E^2_{1/2}$ of

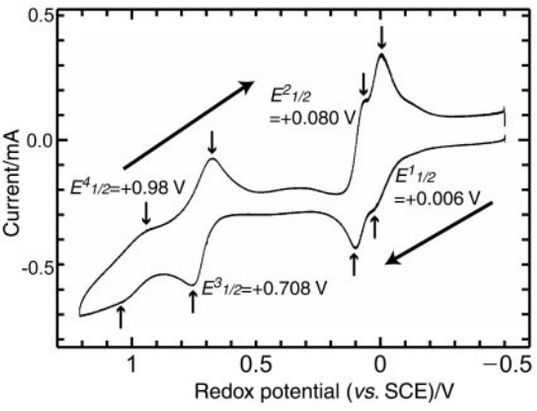

Fig. 2 Cyclic voltammogram of TDAP in 0.1 M $TBA{\cdot}BF_4$, CH_3CN, Pt electrodes, *vs.* SCE, scan speed 10 mV s^{-1}. Peaks are indicated by thin arrows.

Table 1 Cyclic voltammetry data of TDAP under different conditions (at 20–22 °C)

Electrolyte	Electrode			Solvent,[a] scan speed/mV s^{-1}	Redox potentials[b]/V				
	Ref.	Working	Counter		$E^1_{1/2}$	$\Delta E^1 \times 10^{-3}$	Ref.	$E^2_{1/2}$	$\Delta E^2 \times 10^{-3}$
0.1 M TEA·ClO_4	SCE	Glassy carbon	Pt	AN, 50	−0.12	*ca.* 30	−0.05	*ca.* 30	13
0.1 M TBA·BF_4	SCE	Pt	Pt	AN, 10	+0.006	26	+0.080	32	This work
				AN, 100	+0.018	28	+0.083	38	
0.1 M TEA·ClO_4	SCE	Pt	Pt	AN, 10	-0.015	30	+0.052	20	This work
				AN, 100	−0.019	38	+0.052	24	
0.1 M TEA·ClO_4	SCE	Glassy carbon	Pt	AN, 50	−0.045	36	+0.024	20	This work

[a]AN: acetonitrile. [b]$E^1_{1/2}$, $E^2_{1/2}$: average of oxidation and reduction peak potentials, ΔE: difference of the oxidation and reduction peak potentials.

TDAP; $\Delta E^{12} = 0.06$–0.07 V, is extremely small compared to those of common donor or acceptor molecules, *i.e.*, $\Delta E^{12} = 0.37$, 0.24 and 0.55 V for TTF, BEDT-TTF and TCNQ, respectively. This propensity of TDAP to release four electrons very easily by two successive redox steps is one of the most distinctive features of TDAP and is indicative of the extremely weak electron correlation in this molecule.

Two-electron transfer at one redox process has been reported for 2,3,5,6-tetramethyl-TCNQ (Me_4TCNQ),[16] tetracyano-9,10-anthraquinodimethane (TCAQ),[17] 1,2,4,5-tetrakis(dimethylamino)benzene,[18] and 9,10-bis(1,3-dithiol-2-ylidene)-9,10-dihydroanthracene.[19] For all of these compounds the two-electron process has been attributed to their peculiar molecular conformation, for example, the dicyanomethylene groups are almost orthogonally related to each other due to the steric effect in the former two quinodimethanes,[16,17] the neighboring dimethylamino groups are twisted and the aromaticity is lost in the six-membered ring in the amine[18] and the dithiole rings are out of the molecular plane in the neutral and cation states in the anthracene system.[19] In this context it is of interest to study the molecular shape of TDAP, especially the conformation of the dimethylamino groups (see section 4).

A simple estimation of donor strength based on the redox potentials (*vs.* SCE, CH_3CN, 0.1 M TBA·BF_4, Pt) predicts that TDAP ($E^1_{1/2} = +0.02$ V) is a stronger donor than TMTTF (+0.30 V), *N*,*N*-dimethyldihydrophenazine (Me_2P, +0.19 V) and *N*,*N*,*N*′,*N*′-tetramethyl-*p*-phenylenediamine (TMPD, +0.15 V) according to eqn. (3).

$$I_p(D) \propto eE^1_{1/2} + C_1 \quad (3)$$

In eqn. (3) I_p(D) is an ionization potential of electron donor molecules and C_1 includes the terms of solvation energy and electrode potential. However, care should be taken in such estimations, since the molecular size and shape are different from each other and the redox process of TDAP involves two-electron transfer contrary to one-electron transfer for others.

3.2 CT absorption band

The CT transition energy of the *s*-trinitrobenzene (TNB) complex in $CHCl_3$ has been employed as a measure of the donor strength according to eqn. (4),

$$h\nu_{CT}(D{\cdot}TNB) = I_p(D) - E_A(TNB) - C_2 \quad (4)$$

In eqn. (4) E_A(TNB) and C_2 are electron affinity of TNB and mainly Coulomb energy of the CT complex, respectively. The $h\nu_{CT}$(D·TNB) value of TDAP (13.2×10^3 cm^{-1}) indicates that TDAP is a stronger donor than TMTTF (13.9×10^3 cm^{-1}), Me_2P (14.2×10^3 cm^{-1}) and TMPD (15.7×10^3 cm^{-1}) in accordance with the results of the $E^1_{1/2}$ values.

In Fig. 3 the relations between the CT transition energies of TNB complexes in $CHCl_3$ ($h\nu_{CT}$(D·TNB)) and the redox potentials ($E^1_{1/2}$) of several conventional electron donors with planar molecular planes are compared. Accordingly, the donor molecules can be classified into three systems: (**1**) TTF and thiapyrene system, (**2**) azine and benzidine system including TDAP, and (**3**) *p*-phenylenediamine system. Each system exhibits individual relation between the $E^1_{1/2}$ (in V units) and $h\nu_{CT}$(D·TNB) (in 10^3 cm^{-1} units) values as shown in eqns. 5–7 where γ is the correlation coefficient.

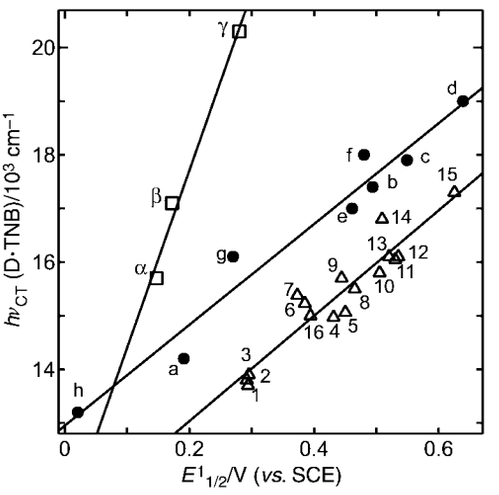

Fig. 3 CT transition energies of *s*-trinitrobenzene (TNB) complexes in $CHCl_3$ ($h\nu_{CT}$(D·TNB)) *vs.* redox potentials ($E^1_{1/2}$) of several conventional strong electron donors with a planar molecular plane. System **1**: 1, hexamethylene-TTF; 2, octamethylene-TTF; 3, TMTTF; 4, bis(ethylenedioxy)-TTF; 5, tetramethytetraselenafulvalene; 6, ethylenedioxy-TTF; 7, TTF; 8, ethylenedioxy-ethylenedithio-TTF; 9, ethylenedithio-TTF; 10, bis(ethylenedioxy)-dibenzoTTF; 11, bis(ethylenedithio)-TTF; 12, bis(heptamethylenethio)-ethylenedithio-TTF; 13, tetrakis(methylthio)-TTF; 14, tetraselenafulvalene; 15, dibenzo-TTF; 16, 1,6-dithiapyrene; System **2**: a, *N*,*N*-dimethyldihydrophenazine (Me_2P); b, dibenzo[*c*,*h*]phenothiazine; c, benzo[*c*]phenothiazine; d, phenothiazine; e, *N*,*N*,*N*′,*N*′-tetramethylbenzidine; f, 3,3′,5,5′-tetramethylbenzidine; g, 1,6-diaminopyrene; h, TDAP; System **3**: α, TMPD; β, diaminodurene; γ, *p*-phenylenediamine. Lines are obtained by least squares method.

$$\text{System 1}: h\nu_{CT}(D{\cdot}TNB) = 9.83\,E^1_{1/2} + 11.1 \ (\gamma = 0.942 \text{ for 16 donors}) \quad (5)$$

$$\text{System 2}: h\nu_{CT}(D{\cdot}TNB) = 9.40\,E^1_{1/2} + 13.0 \ (\gamma = 0.979 \text{ for 8 donors}) \quad (6)$$

$$\text{System 3}: h\nu_{CT}(D{\cdot}TNB) = 33.10\,E^1_{1/2} + 11.1 \ (\gamma = 0.992 \text{ for 3 donors}) \quad (7)$$

The systems **1** and **2** have similar slopes as shown in Fig. 3, but the *p*-phenylenediamine **3** has a remarkably different slope. Therefore, Fig. 3 demonstrates that it is not adequate to compare donor strength of TDAP with that of TMPD and even with those of the TTF systems in terms of the redox

potentials and CT bands. It should be emphasized here that an appropriate comparison of donor strength by the aid of redox potential or CT transition energy is only possible among the same kind of donor molecules in respect of the molecular size, shape and polarizability.[1b,20] However, TDAP displayed much lower $E_{1/2}$ and $h\nu_{CT}$ values than any other donors in Fig. 3 indicating that TDAP is a stronger electron donor than the conventional ones including TMPD, Me_2P and any TTF derivatives.

4 Preliminary results on molecular and crystal structures and molecular orbital calculations

The single crystals for structural analysis were only obtained by the sublimation method. Tiny single crystals were obtained on Teflon sheet by gradient sublimation under low vacuum, though the quality of the crystals was not good enough. The TDAP molecule crystallizes in the triclinic system, $P\bar{1}$ with the following lattice parameters; $a=9.349(2)$, $b=12.953(2)$, $c=9.294(2)$ Å, $\alpha=105.86(1)$, $\beta=98.57(2)$, $\gamma=107.58(2)^\circ$, $V=998.6(4)$ Å^3, $Z=2$, $R=0.111$. Even though the final R-value is still large, the following essential features for the molecular structure and packing pattern of TDAP can be concluded.

Fig. 4 shows the molecular structures of crystallographically independent TDAP molecules, A and B. The atomic numbering scheme of TDAP for structural analysis and MO calculation (Figs. 4 and 5) is different from that for the nomenclature given in Fig. 1. The bond lengths and angles are presented in the supplementary table.† The molecular plane is flat except for one methyl group from each of the dimethylamino groups (Fig. 4a). The TDAP molecule has an inversion at the center of the pyrene moiety. Therefore, the methyl groups residing out of the molecular plane by about 1.4–1.5 Å are related to each other with *cis*-configuration for the dimethylamino groups at C4 (C24a) and C6a (C26) or C4a (C24) and C6 (C26a). The dihedral angle between the averaged molecular plane, *i.e.* the best plane for the pyrene skeleton and the nitrogen atoms, and the dimethylamino groups extending out of the plane is 59° or 63°.

The dihedral angle between the averaged molecular planes of two neighboring TDAP molecules is *ca.* 114° as shown in Fig. 4b. The packing pattern resembles not that of pyrene[21] but that of benzene.[22]

Fig. 5a shows the coefficients of the HOMO and 2nd HOMO of TDAP calculated from the molecular structure in Fig. 4 by AM1 (RHF). Since the crystallographically independent TDAP molecules A and B show very similar molecular conformation, the calculated MO based on each molecule affords no significant differences between them. It is noticeable that the HOMO has C_i symmetry and the coefficients on C5, C5a, C8, and C8a or C25, C25a, C28 and C28a are negligible just like pyrene. Furthermore, it is noted that the HOMO coefficients on the other ring carbon atoms are significantly large compared with those on nitrogen atoms.

The molecular orbital calculation indicates no degeneracy of both HOMO and 2nd HOMO and a sizable energy separation (>1.2 eV) between them. Those results are completely inconsistent with the experimental observations on the redox properties of TDAP.

One of the plausible situations to account for the peculiar redox behaviors is that the molecular structure of $TDAP^0$ in CH_3CN in solution is different from that in the solid. Accordingly the molecular orbital and energy were calculated by AM1 by taking into account the optimization of the molecular geometry. The optimization, however, did not obviously change both the molecular geometry and coefficients from those in Fig. 5a, though the calculated heat of formation was reduced from *ca.* 1400–2000 kJ mol^{-1} to *ca.* 500 kJ mol^{-1}. The HOMO shows the nodal plane along the molecular long axis and no degeneracy.

The next plausible scenario is that the release of one electron by an adiabatic redox process may distort the molecular conformation considerably, and an immediate release of a further electron follows. Moreover, the dication may also have a very favorable conformation for further two-electron release.

In order to verify this scenario, the optimized molecular conformations of the charged species of the TDAP molecule were calculated as shown in Fig. 5b and Table 2. As expected the optimized conformations of $TDAP^{+n}$ ($n=1$–4) show twisted forms around the flat central naphthalene moiety (Plane 2). The two dimethylamino groups linked to a benzene moiety form a flat 1,3-bis(dimethylamino)allyl group (Planes 1 and 3) as clearly recognized in Fig. 5b. Table 2 summarizes the dihedral angles between the planes of the bis(dimethylamino)allyl group and that of the naphthalene moiety. The dihedral angle is 2.2–2.3°, 14.1–14.8° and 22.8° for neutral TDAP and its monocation and dication, respectively. The higher the cationic charge of TDAP from $n=0$ to 2, the greater distortion of the benzene ring attached by two dimethylamino groups. A further increase of n does not seem to affect the conformation.

The easy release of four electrons by two sequential redox steps within a narrow range of redox potentials may occur as follows. On releasing one electron, the optimum orientation for

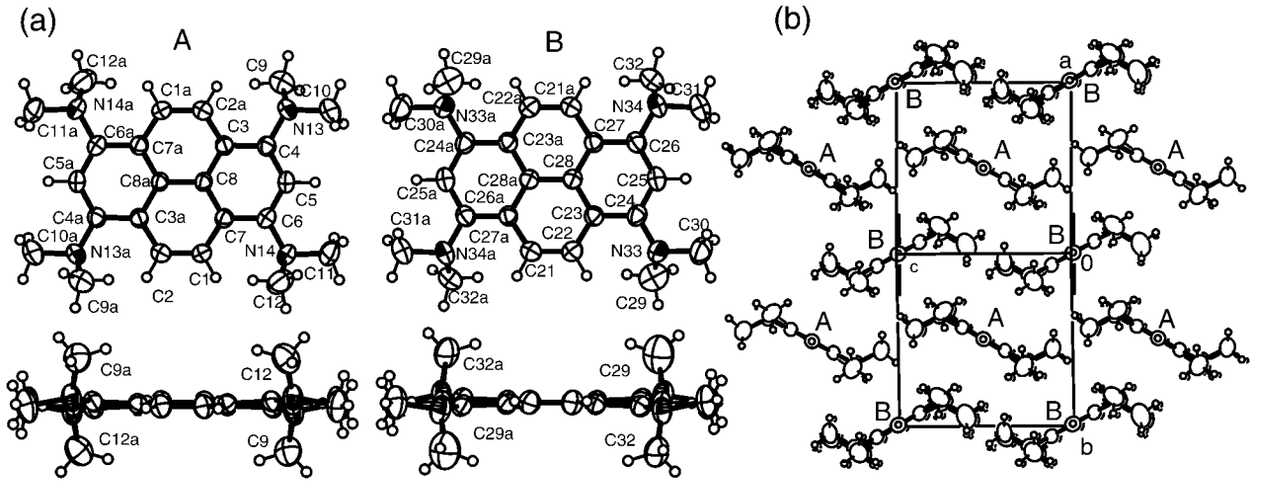

Fig. 4 a) Atomic numbering scheme and molecular structures of crystallographically independent TDAP molecules A and B and b) their crystal structure.

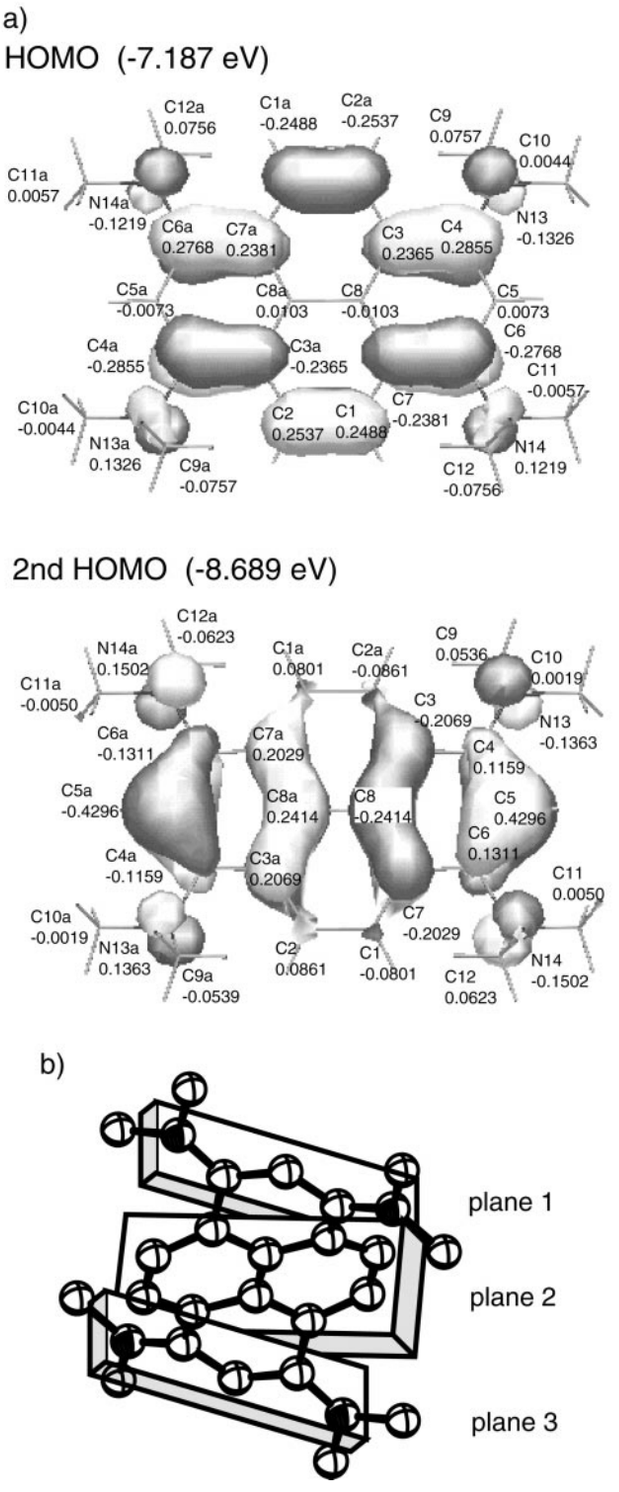

Fig. 5 a) HOMO and second HOMO coefficients and energies of TDAP calculated by AM1 based on the observed molecular structures. Energies are presented in parentheses. b) Schematic view of optimized molecular geometry of $TDAP^{+n}$ ($n = 0$–4). The dihedral angles between the naphthalene moiety (Plane 2) and the bis(dimethylamino)allyl groups (Planes 1 and 3) are summarized in Table 2.

the dimethylamino groups and the central aromatic part may become much more coplanar since the mesomeric stabilization between them enforces the parallel alignment of the p_z-orbitals. This causes steric repulsion between the peri-hydrogen atom of the central naphthalene moiety and the dimethylamino groups and results in a twisted conformation between the naphthalene moiety and the bis(dimethylamino)allyl group. An increase in the ring distortion of the benzene ring will result in diminished aromaticity, and each bis(dimethylamino)allyl group will

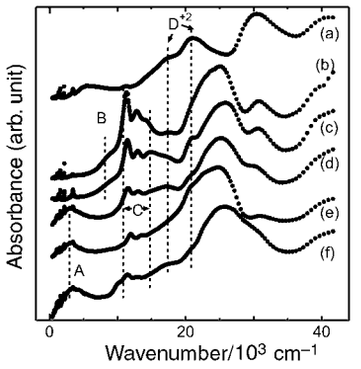

Fig. 6 UV–Vis–NIR spectra of TDAP complexes in KBr with a) F_4TCNQ (1 : 1), b) CF_3TCNQ (1 : 2), c) TCNQ (1 : 2), d) Me_2TCNQ (1 : 2), e) $(MeO)_2TCNQ$ (1 : 3) and f) TCNQ (1 : 4). As for bands A, B, C and D^{+2}, see text.

become more independent, both sterically and electronically, of the other bis(dimethylamino)allyl groups resulting in two-electron transfer. The low ΔE^{12} value of TDAP is reasonably understandable taking into account the redox unit of the bis(dimethylamino)allyl group, the dication of which has a large resonance stabilization.

5 Complex formation

Most of the solid complexes were prepared as powders. The elemental analysis and IR spectra indicate that many of them contain water molecules, which presumably come from moisture. Tables 3, 4 summarize the results: acceptor molecule (A) with its first redox potential ($E^1_{1/2}$(A)), solvent for complex formation, stoichiometry (D : A : solvent), C≡N stretching frequencies of A^0, A^{-1} and the complex, absorption peaks in the UV–Vis–NIR spectra as KBr pellets, electrical conductivity at RT and activation energy for conduction. The complexes are arranged according to the redox potentials of acceptor molecules in Tables 3 and 4 for the TCNQ system, quinone and other kinds of acceptors, respectively. Since almost all products were powders, no structural analysis was available to identify the kinds of species in the compounds. Therefore the characterization of the component species was carefully carried out using all the information available from the elemental analysis, UV–Vis–NIR and IR spectra, conductivity and magnetic data. The component species thus deduced are summarized in the last column of each table.

5.1 Complex of TCNQ system

The strongest acceptor in the TCNQ system in this work, F_4TCNQ provides a 1 : 1 stoichiometry. The major ratio is 1 : 2 in the complexes of TCNQs ranging from CF_3TCNQ to TCNNQ in Table 3. The 1 : 2 complexes are divided into two groups based on their electronic structures, namely, the complex composed of stronger acceptors in the TCNQ system than Et_2TCNQ has a completely ionic ground state, while that composed of weaker acceptors in the TCNQ system than MeTCNQ has a partial CT one. Much weaker ones mainly afford the 1 : 3 complexes with partial CT state. In addition, pristine TCNQ affords a 1 : 4 complex with partial CT state.

Table 2 Dihedral angles (°) between the central naphthalene moiety (Plane 2 in Fig. 5) and bis(dimethylamino)allyl groups (Planes 1 and 3 in Fig. 5)

	$TDAP^0$	$TDAP^{+1}$	$TDAP^{+2}$	$TDAP^{+3}$	$TDAP^{+4}$
Planes 1 and 2	2.3	14.8	22.8	17.8	24.1
Planes 2 and 3	2.2	14.1	22.8	24.7	24.3

Table 3 Stoichiometry, optical and conductivity data of TDAP complexes together with redox potentials of TCNQs

Acceptor[a] ($E^{1}_{1/2}$/V)	Solvent[b]	D : A : solvent	IR(KBr) $\nu_{C\equiv N}$/cm^{-1}			UV–Vis–NIR (KBr)/10^3 cm^{-1}							σ_{RT}/S cm^{-1} (ε_a/meV)	Species
								C			D^{+2}			
			A^0	Complex	A^{-1}	A	B	Band 1	Band 2	Band 3	Band 1	Band 2		
F_4TCNQ (0.60)	AN	1 : 1 : 0.5H_2O	2227 2213	2164s 2132s 2126sh	2212 2193			11.3			18.2	21.3	24.0sh	2.3×10^{-7} (470)	D^{+2}, A^{-2}
CF_3TCNQ (0.44)	Bz+AN	1 : 2 : 0.9H_2O	2223	2185s 2163w	2201 2191 2178		9–10sh	11.3	13.0	14.1	17.8		24.0sh	$<10^{-9}$	D^{+2}, A^{-1}
F_2TCNQ (0.41)	Bz+AN	1 : 2 : 0	2230 2219	2189s 2171w	2205 2182		9-10sh	11.5	13.2	14.5		21.0sh	25.5	$<10^{-9}$	D^{+2}, A^{-1}
FTCNQ (0.32)	PhCl	1 : 2 : 0	2221 2216	2188s 2182sh 2168w	2200 2187 2179		9-10sh	11.5	13.4	14.5		21.0sh	25.5	$<10^{-9}$	D^{+2}, A^{-1}
TCNQ (0.22)	AN	1 : 2 : 0.3H_2O	2225 2222	2179s 2158w	2196 2182 2167		9-10sh	11.5	13.0	14.9	16.7	21.2sh	25.9	$<10^{-7}$	D^{+2}, A^{-1}
	PhCl	1 : 4 : 0	2225 2222	2198s 2178s 2157s 2131sh	2196 2182 2167	3.5	10sh	11.5	13.0		17.8sh	25.8		3.6×10^{-1} (72)	D^{+2}, H_nD^{+n} $A^{-(2-\gamma)}$, $A^{-(1-\delta)}$ $\delta, \gamma \sim 0$
C_{10}TCNQ (0.21)	Bz	1 : 2 : 1.5Bz	2222	2176s 2157sh	2185 2172		9-10sh	11.5	13.1	14.6	17.4	21.3sh	24.6	4.2×10^{-7} (200)	D^{+2}, A^{-1}
MeTCNQ (0.19)	Bz	1 : 2 : 0.3H_2O	2223	2178s 2159sh	2189 2172		9-10sh	11.6	13.1	14.9	17.4	21.0sh	24.9	1.9×10^{-7} (350)	D^{+2}, A^{-1}
Et_2TCNQ (0.15)	AN	1 : 2 : 1H_2O	2213	2176 2151	2184 2155	3.3	6.6	11.6	13.1	15.3	17.4	21.3	24.0	3.0×10^{-1} (90)	$D^{+2(1-\delta)}$, $A^{-(1-\delta)}$ $\delta \sim 0$
Me_2TCNQ (0.15)	Bz+AN	1 : 2 : 0.5H_2O	2222 2210	2176s 2156w	2183 2164	3.1		11.5	13.1		17.2	21.0	25.1	2.2 (77)	$D^{+2(1-\delta)}$, $A^{-(1-\delta)}$ $\delta \sim 0$
TCNNQ (0.07)	Bz+AN	1 : 2 : 0.5H_2O	2224	2177s 2159sh	2192 2178	3.3	9.0	12.1	13.4		17.6sh	21.2		1.5 (75)	$D^{+2(1-\delta)}$, $A^{-(1-\delta)}$ $\delta \sim 0$
$(MeO)_2$TCNQ (0.05)	PhCl	1 : 3 : 0.5H_2O	2219	2222w 2178s 2159s	2198 2175	3.1		12.0	13.4			21.0sh	24.8	$1.8\times10-1$ (67)	$D^{+(2-2\delta+\gamma)}$ $A^{-(1-\delta)}$, $A^{-\gamma}$ $\delta, \gamma \sim 0$
BTDA-TCNQ (0.03)	PhCl	1 : 3 : 0	2230	2215w 2183s	2206 2191	2.9	8.8			15.3sh	17.2sh	22.0	25.1	6.5×10^{-2} (52)	$D^{+(2-2\delta+\gamma)}$ $A^{-(1-\delta)}$, $A^{-\gamma}$ $\delta, \gamma \sim 0$
$(EtO)_2$TCNQ (0.01)	Bz+AN	1 : 3 : 0	2221	2213w 2179s 2159w	2185 2167	3.9		11.8	13.4	15.1	17.4sh		23.8	9.0×10^{-2} (110)	$D^{+(2-2\delta+\gamma)}$ $A^{-(1-\delta)}$, $A^{-\gamma}$ $\delta, \gamma \sim 0$

[a] $E^{1}_{1/2}$: average of oxidation and reduction peak potentials, *vs.* SCE, TBA·BF_4, acetonitrile, Pt electrode, 10–100 mV s^{-1}, 20–22 °C. [b] Bz: benzene, AN: acetonitrile, PhCl: chlorobenzene.

Table 4 Stoichiometry, optical and conductivity data of TDAP complexes together with redox potentials of quinones and miscellaneous acceptor molecules

Acceptor[a] ($E^{1}_{1/2}$ /V)	Solvent[b]	D : A : solvent	IR(KBr)$\nu_{C\equiv N}$/cm^{-1}			UV–Vis–NIR (KBr)/10^3 cm^{-1}					σ_{RT}/S cm^{-1} ε_a/meV	Species
						B		D^{+2}				
			A^0	Complex	A^{-1}							
DDQ (0.56)	Bz	1 : 2 : 0.8H_2O	2234	2214	2217	13.4		18.5sh	21.5	24.3	$<10^{-9}$	D^{+2}, A^{-1}
DBDQ (0.54)	Bz	1 : 2 : 1.1H_2O	2230	2215	2214	12.8		18.2sh	21.3	24.1	$<10^{-9}$	D^{+2}, A^{-1}
DIDQ (0.51)	Bz	1 : 2 : 0.8H_2O	2226	2208	2209	12.8		18.0sh	21.5sh	23.8	$<10^{-9}$	D^{+2}, A^{-1}
DCNNQ (0.38)	PhCl	1 : 2 : 0	2234	2198	2200	12.8		18.5sh	21.4	24.5sh	$<10^{-9}$	D^{+2}, A^{-1}
DCNQ (0.21)	Bz	1 : 2 : 0.7H_2O	2236 2225	2196	2206	14.1		17.7sh	21.2	24.3sh	$<10^{-9}$	D^{+2}, A^{-1}
QCl_4 (0.05)	Bz	1 : 1.8 : 3H_2O						18.2sh	21.9	24.8sh	$<10^{-8}$	D^{+2}, D^0, A^{-1}, A^0
QBr_4 (0.04)	Bz	1 : 1.8 : 3H_2O						17.7sh	21.7	24.9sh	$<10^{-9}$	D^{+2}, D^0, A^{-1}, A^0
QF_4 (0.04)	Bz	1 : 1.8 : 3H_2O				12.8sh	15.5sh	18.1sh	22.5		$<10^{-9}$	D^{+2}, D^0, A^{-1}, A^0
QI_4(−0.02)	Bz	1 : 1.7 : 2H_2O						18.0sh	21.8sh		$<10^{-9}$	D^{+2}, D^0, A^{-1}, A^0
2,5-QCl_2 (−0.15)	Bz	2 : 5 : 4H_2O						17.4sh	21.3		$<10^{-9}$	D^{+2},D^0,A^{-1}, A^0
Cl_2NNQ (−0.20)	Tol	~2 : 3 : 4H_2O					15.2sh	17.4sh	22.4		—	D^{+2}, A^{-1}, A^0
I_3 (0.64)	Bz	1 : 2.1						17	22	26	$<10^{-9}$	D^{+2}
TCNE (0.29)	Bz+	1 : 2.5 : 2H_2O : 1Bz	2262	2200	2201		12.8sh	17.8sh	21.7sh	23.7	1.6×10^{-7} (510)	D^{+2}, A^{-1}
	AN		2228	2173								
DTENF (0.23)	Bz+	1 : 2 : 1.9AN	2233	2182	2190	9.4sh	12.0	17.7	21.5	25.0	$<10^{-9}$	D^{+2}, A^{-1}
	AN		2160									
DTNF (0.02)	Bz+	1 : 2 : 0	2230	2182	2203	10.3sh	12.9	17.6	22.1	26.3sh	8.0×10^{-7} (390)	D^{+2}, A^{-1}
	AN		2151	2186								
TENF (−0.14)	Tol	1 : 1 : 0				7.5		17.0sh	23.4			D^0, A^0
TNF (−0.43)	Tol	1 : 1 : 0				9.0			23.1			D^0, A^0
C_{60} (−0.44)	Bz	1 : 2 : 1Bz				11.4		16.6sh	23.5		$<10^{-9}$	D^0, A^0
TNB (−0.56)	Bz	1 : 1 : 0.2H_2O				12 ~ 13			23.4			D^0, A^0

[a] $E^{1}_{1/2}$: average of oxidation and reduction peak potentials, *vs.* SCE, TBA·BF_4, acetonitrile, Pt electrode, 10–100 mV s^{-1}, 20–22 °C. [b] Bz: benzene, AN: acetonitrile, PhCl: chlorobenzene, Tol: toluene.

5.1.1 1 : 1 $D^{+2}A^{-2}$ complex. The F_4TCNQ molecule afforded a 1 : 1 complex. The complex exhibits two C≡N stretching modes (2164, 2132 cm^{-1}) which are lower by 50–60 cm^{-1} compared with those of K·F_4TCNQ (2212, 2193 cm^{-1}). This indicates that the bond order of C≡N in F_4TCNQ in the TDAP complex is decreased compared with the monoanion of F_4TCNQ and the complex is most plausibly formulated as ($TDAP^{+2}$)(F_4TCNQ^{-2}). CT complexes with the dianion of F_4TCNQ are rare and only a few examples have been found, such as those with decamethylferrocene,[23] hexaazaoctadecahydrocoronene,[24] and tris(1,2-benzothio)trimethylenemethane.[25] The assignment of the dianion state of F_4TCNQ in the TDAP complex corresponds well with the observation of the corresponding C≡N modes at 2167 and 2133 cm^{-1} in (decamethylferrocene^{+2})(F_4TCNQ^{-2}).

The UV–Vis–NIR absorption spectrum of the F_4TCNQ complex in a KBr pellet (curve a in Fig. 6) consists of bands at *ca.* 18 (shoulder) and 21.3×10^3 cm^{-1}, which can be attributed to $TDAP^{+2}$ (denoted band D^{+2}), but not to the protonated species of TDAP (see 5.1.4). A small peak at 11.3×10^3 cm^{-1} is due to contamination with the monoanion of F_4TCNQ as an impurity. Some samples exhibit a weak broad band at 5.7×10^3 cm^{-1} the origin of which is unknown.

The observed static magnetic susceptibility after subtracting Pascal diamagnetism shows Curie behavior down to 2 K with spin concentration of 0.4% of complex. The EPR measurements at RT showed two Lorentzian signals with the same *g* value of 2.0037. Both signals account for *ca.* 0.1% of the spin concentration of the complex. These results indicate that the observed spins are not intrinsic ones but are ascribed to defects or impurities.

A σ-bond formation has been reported for the complex formation between TMPD and F_4TCNQ.[26] In the case for TDAP and F_4TCNQ, however, no such reaction was detected in acetonitrile or chlorobenzene probably owing to the difference in molecular size between them.

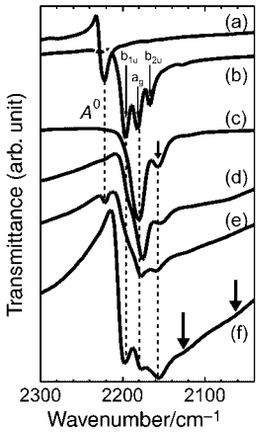

Fig. 7 IR spectra in KBr of c) 1 : 2 TCNQ, d) 1 : 2 Me_2TCNQ, e) 1 : 3 $(MeO)_2TCNQ$ and f) 1 : 4 TCNQ complexes of TDAP are compared with those of a) neutral TCNQ and b) K·TCNQ. For arrows, see text.

5.1.2 1 : 2 fully ionic $D^{+2}(A^-)_2$ complex. The 1 : 2 CF_3TCNQ, F_2TCNQ, FTCNQ, TCNQ, $C_{10}TCNQ$ or MeTCNQ complexes show similar UV–Vis–NIR spectra to each other. They exhibit characteristic multiple bands between 10 and 15×10^3 cm^{-1} (labeled band C in Fig. 7) and are assigned to the intramolecular anion radicals of TCNQs.[27] In Fig. 6 the spectra of the CF_3TCNQ (curve b) and TCNQ (1 : 2 phase, curve c) complexes are presented as examples. A shoulder is observed at $9–10\times10^3$ cm^{-1} for all of them. These bands originate from the optical transition between anion radical molecules (labeled band B)[27] and are related to the effective *U*. Therefore it is evident that the anion radical molecules of the acceptor molecule form segregated columns. No optical transition for the partial CT state of acceptor molecules, namely a band below 5×10^3 cm^{-1} (labeled band A),[27] is observed. Consequently, the complex is formulated as

$(D^{+2})(A^{-})_2$ with segregated stacks constructed by fully ionized species. The absence of both bands B and C in the spectrum of $(TDAP^{+2})(F_4TCNQ^{-2})$ differentiates it from $(TDAP^{+2})(A^{-})_2$.

In Fig. 7 the IR spectrum of the 1 : 2 TCNQ complex (curve c), as an example, is compared with those of neutral TCNQ (curve a) and of K·TCNQ (curve b) in KBr. It is noticeable that the first C≡N stretching band observed in K·TCNQ (b_{1u}, 2196 cm^{-1}) is missing in the 1 : 2 TDAP complex. The first C≡N band in the TDAP complex (2179 cm^{-1}) has almost the same frequency as that of the a_g mode of K·TCNQ (2182 cm^{-1}).[9a,28] Such an optical feature is commonly observed in the complexes in this class. The strong peak due to the a_g mode indicates a large distortion of the TCNQ segregated column. In addition, the TDAP complexes exhibited either C≡N stretching modes at lower frequencies (for CF_3TCNQ, TCNQ) or additional modes at low frequencies (for F_2TCNQ, FTCNQ, $C_{10}TCNQ$, MeTCNQ) compared to those in the potassium or lithium salt of corresponding TCNQ (see Table 3). As an example, the band indicated by arrow (2158 cm^{-1}) in curve c is considerably down shifted compared to that in K·TCNQ (2167 cm^{-1}, b_{2u}). These results suggest either that the charge of TCNQ species is more than −1 or that specific atomic contacts between the C≡N group of $TCNQ^{-1}$ and $TDAP^{+2}$ exist and decrease the bond order of the C≡N bond, though no structural information is available. However, the absence of the band A rules out the former case. Similar down shift of the C≡N modes has been reported in [*N*,*N*′-ethylenebis(acetylacetoniminato) Co(II){-Co(acacen)}(pyridine)$_2$]($TCNQ^{-1}$), where the $\nu_{C\equiv N}$ appears at 2171 and 2145 cm^{-1}.[29] Therefore, no linear relationship is expected between $\nu_{C\equiv N}$ of the IR spectrum and the degree of CT in the system studied here contrary to that in the conventional TCNQ complexes.[30]

The completely ionized nature in both the donors and acceptors is compatible with the insulating conductivity of these complexes.

The static spin susceptibility of the F_2-, F-, Me- and TCNQ complexes showed Curie behavior with a Curie constant of 2.9×10^{-3}–1.9×10^{-2} emu mol^{-1} or *ca.* 0.3–5% of complex. Though the spin quantity of some complexes is too high to be caused by a Curie impurity, the subtraction of the Curie term revealed the singlet–triplet excitation mechanism expressed by eqn. (8),[31] where χ_0, C, N, μ_B and k_B are the Pascal diamagnetism, Curie constant, Avogadro's number, Bohr magneton and Boltzmann constant, respectively.

$$\chi_p=\chi_0+C/T+(2Ng^2\mu_B^2/k_BT\{1/[3+\exp(2J/k_BT)]\} \quad (8)$$

The energy gap between the singlet ground state and triplet excited state is roughly calculated as $2J/k_B = ca.\ -780$ K for the F_2TCNQ complex. For the other complexes, only a slight increase of $(\chi_p-\chi_0-C/T)$ is observed above 250 K and so a reliable $2J$ value is not evaluated. The spins of the TCNQs segregated stack are strongly coupled antiferromagnetically in this class of complex.

5.1.3 Partial CT complex. The complexes in this class reveal both a low-energy optical transition below 5×10^3 cm^{-1} (band A) and high electric conductivity. The complex of Et_2TCNQ, Me_2TCNQ or TCNNQ has a 1 : 2 stoichiometry. $(MeO)_2TCNQ$, BTDA-TCNQ or $(EtO)_2TCNQ$ affords a 1 : 3 complex. TCNQ provides even a 1 : 4 complex in addition to the insulating 1 : 2 one above mentioned.

The UV–Vis–NIR spectra of 1 : 2 Me_2TCNQ, 1 : 3 $(MeO)_2TCNQ$ and 1 : 4 TCNQ complexes are presented by curves d, e and f, respectively, in Fig. 6. The presence of band A indicates both partial CT state and segregated stack of the constituent molecules. In the 1 : 4 complex band B is observed at around 10×10^3 cm^{-1}. The dull multiple bands at 11–15×10^3 cm^{-1} (band C) confirms the existence of anion radical molecules of acceptor.

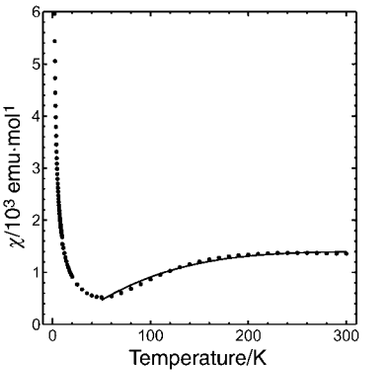

Fig. 8 Temperature dependence of the magnetic susceptibility of 1 : 4 TCNQ complex after correction of core diamagnetism. The solid line indicates a 1D Heisenberg alternate chain model with $|J|/k_B = 258$ K and $\alpha = 0.85$ above 50 K.

The partial CT state in the 1 : *n* [*n* = 2, 3, 4] complex requires that the acceptor part is not monoanion but less than −1, namely $-(1-\delta)$ and TDAP is $+n(1-\delta)$ [$\delta>0$, $n=2, 3, 4$], if the charge is shared equally among the component species. The charge sharing among the constituent molecules was examined by the IR spectra especially in the C≡N stretching region for the TCNQs. Fig. 7 compares the C≡N stretching modes of the 1 : 2 Me_2TCNQ (curve d), 1 : 3 $(MeO)_2TCNQ$ (curve e) and 1 : 4 TCNQ (curve f) complexes and the characterization of the chemical species in the acceptor part is described below.

Owing to the partial CT state, regardless of whether the charge sharing is uniform or not, a fairly high conductivity ($\sigma_{RT} = 0.07$–2 S cm^{-1}, $\varepsilon_a = 50$–100 meV on compressed pellet samples) was observed in all complexes in this class. However, it is not evident whether the donor part participates in the carrier transport.

5.1.3.1 1 : 2 complex: $(D^{+2(1-\delta)})(A^{-(1-\delta)})_2$ ($\delta\sim0$). These complexes exhibit C≡N stretching modes which are ascribed to one species with a charge close to monoanionic. Therefore, the complex is formulated as $(D^{+2(1-\delta)})(A^{-(1-\delta)})_2$ ($\delta>0$) with segregated stack, where the TDAP molecules are very close to a dication but not exactly $TDAP^{+2}$ nor H_2TDAP^{+2} (see 5.1.4). The first C≡N stretching mode is observed as a weak shoulder at around 2190–2200 cm^{-1} (see curve d in Fig. 7), while that at 2176–2177 cm^{-1}, which is probably characterized as an a_g mode, is observed as a strong peak suggesting a distortion of

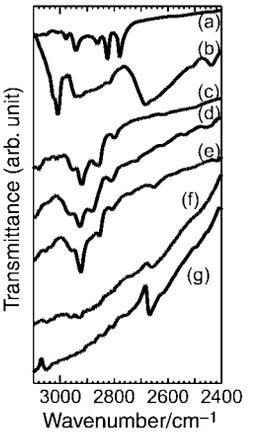

Fig. 9 IR spectra in KBr of TDAP complexes with d) F_4TCNQ (1 : 1), e) TCNQ (1 : 2), f) TCNQ (1 : 4 from chlorobenzene) and g) TCNQ (1 : 4 by diffusion method, CH_3CN + benzene) are compared with those of a) neutral TDAP, b) $(H_4TDAP^{+4})Cl^{-}_4(H_2O)_x$ ($x = 1.5$–2) and c) $(TDAP)(I_3)_{2.1}$.

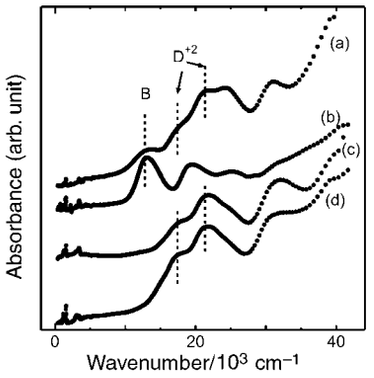

Fig. 10 UV–Vis–NIR spectra in KBr of a) DDQ, c) QCl_4 (*p*-chloranil) and d) 2,5-QCl_2 (2,5-dichloro-*p*-benzoquinone) complexes of TDAP compared with that of b) tetraethylammonium DDQ. As for bands B and D^{+2}, see text.

the segregated column of TCNQs. In the UV–Vis–NIR spectrum, the Et_2TCNQ or TCNNQ complex exhibits band B, while such a band in the Me_2TCNQ complex (curve d Fig. 6) is most likely embedded in the bands A and C.

The temperature dependence of the static magnetic susceptibility was measured for the Me_2TCNQ complex. After subtraction of the Curie impurity, which amounts to as much as *ca.* 3–4% of the complex, the susceptibility shows very slight temperature dependence down to 20 K (2.8–3.7×10^{-4} emu f.u.$^{-1}$). This behavior suggests a Pauli-like susceptibility above 20 K, though a compaction sample shows a semiconductive activation energy of 77 meV for conduction.

5.1.3.2 1 : 3 complex: $(D^{+(2-2\delta+\gamma)})(A^{-(1-\delta)})_2(A^{-\gamma})$ (δ, $\gamma\sim0$). In the 1 : 3 complex of $(MeO)_2$TCNQ, BTDA-TCNQ or $(EtO)_2$TCNQ a weak C≡N stretching mode appears at high frequency (2222 cm^{-1} for the $(MeO)_2$TCNQ complex; curve e in Fig. 7), and is assigned to a species ionized much less than the monoanion and close to a neutral species (2219 cm^{-1} for a neutral species, denoted A^0). The intensity of this mode is very weak compared with the C≡N stretching modes at lower frequencies (2178, 2159 cm^{-1} for the $(MeO)_2$TCNQ complex) which are ascribed to the species close to a monoanion. Although the highly conductive nature of this complex may suggest that the acceptor part shares charge uniformly (close to −2/3), the above IR data clearly reveal the non-uniform charge distribution among the acceptor species, namely the acceptor part is formulated as $(A^{-(1-\delta)})_x(A^{-\gamma})_{3-x}$ (δ, $\gamma\sim0$). This kind of charge separated state has been frequently observed in the 2 : 3 TCNQ complexes such as $Cs_2(TCNQ)_3$.[32]

The presence of band B in the BTDA-TCNQ complex certainly indicates the presence of neighboring $A^{-(1-\delta)}$ species in the solid. While the band B in the $(MeO)_2$TCNQ (curve e in Fig. 6) or $(EtO)_2$TCNQ complex may be embedded in bands A and C.

5.1.3.3 1 : 4 complex. The 1 : 4 complex has only been obtained with pristine TCNQ so far. The mixing of acetonitrile solutions simply affords the insulating 1 : 2 complex. However, the reflux of chlorobenzene solutions of TDAP and TCNQ or crystal growth by the diffusion method gave the 1 : 4 complex. By the diffusion method the 1 : 4 complex is harvested at the acceptor side in the diffusion cell while at the donor side only the 1 : 2 complex was afforded. The UV–Vis–NIR spectra of the TCNQ complexes differ by the presence or absence of the low-energy band below 5×10^3 cm^{-1} in the 1 : 4 or 1 : 2 complex, respectively (curves c and f in Fig. 6).

The IR spectrum in the C≡N region of the 1 : 4 TDAP-TCNQ (curve f in Fig. 7) reveals a very broad absorption between 2200 and 2000 cm^{-1} with three clearly separated peaks at 2198, 2178 (a_g) and 2157 cm^{-1} and two dents at 2131 and 2060 cm^{-1} (indicated by thick arrows in Fig. 7). The peaks at 2198, 2178 and 2157 cm^{-1} should be ascribed to those close to the monoanion state of TCNQ; $TCNQ^{-(1-\delta)}$ ($\delta\sim0$). The presence of a strong a_g mode indicates lattice distortion. The last two modes at 2131 and 2060 cm^{-1} are ascribed to the TCNQ species ionized more than the monoanion. It was reported that a dianion of TCNQ molecules exhibited only two C≡N stretching frequencies at 2151 and 2102 cm^{-1} in the solid state [Co(acacen)(pyridine)$_2$]$_2$TCNQ.[29] Later three peaks at 2190–2205, 2135–2140 and 2060–2100 cm^{-1} were observed in a system of (transition metal: V, Cr, Mo, W, Co or Ni)$(TCNQ)_m(CH_3CN)_n$: $m=1$–2 and $n=0$–2, where the $TCNQ^{-2}$ interacts with the highly polarizable metal center with the C≡N groups.[33] It was noticed that with a symmetrical compound the band at 2135–2140 cm^{-1} disappeared.[33] According to these observations, the presence of the dents at 2131 and 2060 cm^{-1} in the 1 : 4 TDAP complex definitely demonstrates the presence of $TCNQ^{-(2-\gamma)}$ with γ being close to zero and the species are asymmetric. Consequently the TCNQ species in the 1 : 4 complex do not share the charge uniformly but exist as a charge separated state; namely a mixture of $TCNQ^{-(1-\delta)}$ and $TCNQ^{-(2-\gamma)}$: $(TCNQ^{-(1-\delta)})_{3+x}(TCNQ^{-(2-\gamma)})_{1-x}$. It is not conclusive that the $TCNQ^{-(2-\gamma)}$ species are involved in the TCNQ segregated column since the electron transport may have a serious disadvantage if the segregated column consists of a mixture of $TCNQ^{-(1-\delta)}$ and $TCNQ^{-(2-\gamma)}$.

The temperature dependence of the static magnetic susceptibility is presented in Fig. 8 after correction of core diamagnetism. The low temperature region is expressed by the Curie behavior with Curie impurity of *ca.* 1.4 %. The temperature dependence above 150 K is well approximated by a 1D Heisenberg alternate chain model[31] with $|J|/k_B=258$ K and $\alpha=0.85$ assuming 3 spins per formula unit as shown in Fig. 8.

It should be emphasized that the 1 : 4 TCNQ complex studied here is different from the numbers of highly conductive 1 : 4 TCNQ complexes with bipyridyl derivatives so far reported by Ashwell *et al.* since the latter consist of dication species and $(TCNQ^{-0.5})_4$.[34]

5.1.4 Cation species. The molecular species of the cation part of the complexes were examined by their IR spectra in the region of C–H and N–H stretching modes (3100–2400 cm^{-1}, Fig. 9). The neutral TDAP (curve a in Fig. 9) and its tetrakis HCl salt (curve b in Fig. 9) exhibit characteristic bands of tertiary amine and its protonated salt, respectively, in this region. The 1 : 1 F_4TCNQ complex (curve d in Fig. 9) does not exhibit any such bands for both neutral TDAP and protonated TDAP but resembles those of $TDAP^{+2}$ observed in $(TDAP)(I_3)_{2.1}$ (curve c), confirming that the cation species are $TDAP^{+2}$ but not H_2TDAP^{+2}. The 1 : 2 TCNQ (curve e in Fig. 9) complex also exhibits almost the same features as curve c in Fig. 9. This is a strong evidence that the 1 : 2 complex is formulated as $(TDAP^{+2})(TCNQ^{-1})_2$. Such characteristic bands seen in $TDAP^{+2}$ are commonly observed in all the 1 : 2 and 1 : 3 complexes in Table 3 and the cation species is postulated to be $TDAP^{+2(1-\delta)}$ or $TDAP^{+(2-2\delta+\gamma)}$ with γ and δ close to zero.

Curve f in Fig. 9 shows the IR spectrum of the 1 : 4 complex from chlorobenzene. The strong electronic transition (band A, curve f in Fig. 6) extends into this region and precludes any possible identification of the characteristic bands originated from $TDAP^{+2}$ or protonated TDAP. In Fig. 6 we have noticed that the 1 : 4 TCNQ complex from chlorobenzene exhibited bands at *ca.* 18 and 22×10^3 cm^{-1}, which are ascribed to $TDAP^{+2(1-\delta)}$. Although we do not have spectral data on the $TDAP^{+4}$ and H_2TDAP^{+2} species, it is expected that the cationic part of the 1 : 4 complex from chlorobenzene comprises partly $TDAP^{+2(1-\delta)}$.

The 1 : 4 complex formed by the diffusion method from a mixture of CH_3CN and benzene (curve g in Fig. 9) clearly exhibits a broad band at 2668 cm^{-1} (a faint dent is seen at this frequency in curve f in Fig. 9). The appearance of this broad band strongly suggests the presence of the protonated species in the cation part. The UV–Vis–NIR spectrum of this complex is almost identical to that of the 1 : 4 complex from chlorobenzene. Consequently, it is concluded that the cation part of the 1 : 4 complex includes both $TDAP^{+2(1-\delta)}$ and protonated TDAP, H_nTDAP^{+n} ($n=1\sim4$ and in which the exact number n is unknown) and mixed CT species of TCNQ ($A^{-(1-\delta)}$, $A^{-(2-\gamma)}$). Such a complicated mixed state of simultaneous charge- and proton-transfer has also been observed in the biimidazole·TCNQ system.[35]

5.2 Complex of quinone system

With *p*-quinone derivatives, the stoichiometry of donor to acceptor is 1 : 2 for acceptors stronger than *p*-chloranil (QCl_4). The weaker acceptors including QCl_4 afford non-stoichiometric products: the best fit of D : A is 1 : 1.7 for *p*-iodanil (QI_4) and 1 : 1.8 for other *p*-haloanils (fluoranil (QF_4), chloranil, bromanil (QBr_4)). 2,5-Dichloro-*p*-benzoquinone (2,5-QCl_2) affords 2 : 5 stoichiometry.

The UV–Vis–NIR spectra of the complexes of DDQ, DBDQ, DIDQ, DCNNQ and DCNQ resemble each other. They exhibit a weak absorption band at $12–14\times10^3$ cm^{-1} ascribed to the anion radical molecules in a segregated stack (band B). In Fig. 10 the absorption spectrum of $(TDAP)(DDQ)_2(H_2O)_{0.8}$ (curve a) is compared with that of the tetraethylammonium salt of DDQ, TEA·DDQ (curve b) in KBr pellets. The lowest energy band at *ca.* 13×10^3 cm^{-1} (band B) is weakly observed in the TDAP complex. The bands at 18–19 and $21–22\times10^3$ cm^{-1} are ascribed to those of the $TDAP^{+2}$ species.

The comparison of the IR spectrum of the DDQ complex with those of the I_3 salt of TDAP and various kinds of DDQ compounds (neutral DDQ, TEA·DDQ, hydroquinone of DDQ) reveals that the complex is composed of $TDAP^{+2}$ and $DDQ^{-}\cdot$. Similarly other 1 : 2 complexes have the same features. No bands of the protonated TDAP are detected. It is noticeable that the C≡N stretching band in the IR spectrum appears almost the same or at a little lower frequency by 10 cm^{-1} compared to those of the corresponding potassium or alkylammonium salt of the monoanion. In accord with the completely ionized nature, the 1 : 2 complexes of *p*-quinones exhibit insulating conductivity with $\sigma_{RT}<10^{-9}$ S cm^{-1}.

For the *p*-haloanil complexes, the donor part is in a little excess compared with the acceptor part in their stoichiometries of D : A. Both the absence of band A and the insulating nature of the complexes implicate either the alternating stack or the non-partial CT state in the complex. UV–Vis spectra resemble those of $(TDAP^{+2})(F_4TCNQ^{-2})$. As an example, the spectrum of the QCl_4 complex is depicted by curve c in Fig. 10, which shows that the TDAP molecules are in the dicationic state in the complex. However, their stoichiometry, *i.e.* 1 : 1.7 or 1 : 1.8, requires a negative charge on the acceptor of a little more than unity if the donor part is made of only +2 species. However, this is not conceivable since *p*-haloanils have a weaker electron accepting ability than DDQ. As a consequence it is deduced that the excess neutral TDAP molecules are present in the complexes; this is supported by the appearance of several weak bands ascribable to neutral TDAP in the IR spectra. Furthermore, the weak band observed at 1681 cm^{-1} in the QCl_4 complex and 1672 cm^{-1} in the QBr_4 complex confirms the presence of neutral *p*-haloanils, the C=O stretching of which appears at 1680–1690 cm^{-1} and 1672–1681 cm^{-1} for QCl_4 and QBr_4, respectively. Thus the complex includes four different species, namely, D^{+2}, D^0, A^{-1} and A^0. If we assume the commensurate ratio among the component species, the TDAP complex is formulated as $(D^{+2})_a(D^0)_b(A^{-1})_{2a}(A^0)_c$ with three possible sets of a, b, and c for the 1 : 1.8 complex; *i.e.* $a:b:c=4:1:1$, 7 : 3 : 4 or 3 : 2 : 3. Very weak intensity of the C=O stretching together with weak peaks for the neutral TDAP complex exclude the latter two possibilities. The QI_4 complex exhibits an IR band at 1658 cm^{-1} which is assigned to the C=O stretching of neutral QI_4 (1660 cm^{-1}). Hence, this complex is similarly assigned to be composed of four kinds of species, D^{+2}, D^0, A^{-1}, A^0. The lack of band A indicates an alternating stack instead of a segregated one.

Even with a weak electron acceptor, 2,5-QCl_2, TDAP gives an ionic complex which exhibits a UV-Vis spectrum (curve d in Fig. 10) characterized as the highly cationic state of TDAP. The IR spectrum of the complex indicates the coexistence of C=O stretching modes of monoanion (C=O 1569 cm^{-1}) and neutral (C=O 1671 cm^{-1}) species, the former is much more intense. Also the IR bands ascribed to the neutral TDAP are observed in the region of 1500–1000 cm^{-1}. Therefore, the components of the complex are deduced to be D^{+2}, D^0, A^{-1} and A^0. The absence of bands A and B strongly suggests the non-segregated stack.

The weakest quinone which affords solid product is Cl_2NNQ. The UV–Vis and IR spectra of the product in KBr indicate the presence of D^{+2} as well as A^0. Although the stoichiometry by elemental analysis is not determined satisfactorily owing to the poor yield, the product is composed of at least, D^{+2}, A^{-1} and A^0.

5.3 Complex of other acceptors

The TDAP molecule affords ionic complexes of $TDAP^{+2}$ with approximate stoichiometry of 1 : 2 with I_3, DTENF, DTNF and TCNE in accordance with their redox potentials. They exhibit absorption bands at 17–18 and $21–22\times10^3$ cm^{-1} similar to those of the $TDAP^{+2}$ complexes above mentioned. They do not exhibit optical band A. Only the DTENF and DTNF complexes among them show absorption bands at 9–12 and $10–13\times10^3$ cm^{-1}, respectively, which are ascribed to band B indicating the segregated stack of acceptor molecules.

On the other hand, weak acceptors, TENF, TNF, C_{60} and *s*-TNB molecules afford 1 : 1 or 1 : 2 neutral complexes which show conventional CT bands at 7.5, 9.0, 11.4 and 12–13×10^3 cm^{-1}, respectively. Other bands in the UV–Vis spectra

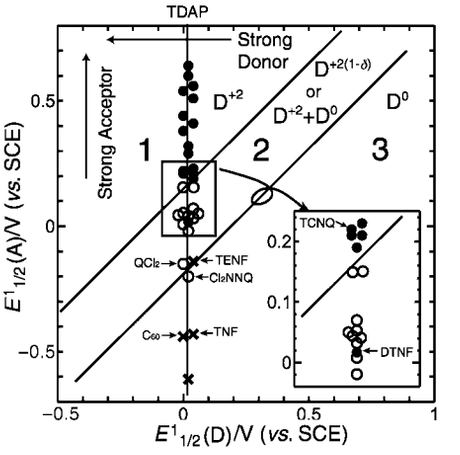

Fig. 11 Ionicity diagram of TDAP ($E^1_{1/2}=+0.02$ V) system. The 1 : n TDAP complexes ($n=1–3$) in the regions **1** (ionic), **2** (partial) and **3** (neutral) are composed of mainly D^{+2} (indicated by closed circle), $D^{+2(1-\delta)}$, $D^{+(2-2\delta+\gamma)}$, $(D^{+2}+A^{-1}+A^0)$ or $(D^{+2}+D^0)$ (open circle) and D^0 (cross), respectively. Some complexes discussed in the text are labeled by the name of the acceptor. Inset shows the expanded part near the upper boundary. Two straight lines represent $\Delta E(DA)$ $(=E^1_{1/2}(D)-E^1_{1/2}(A))=-0.15$ and +0.19 V *vs.* SCE. Although all the points are on the vertical line at $E^1_{1/2}(D)=+0.02$, they are depicted at horizontally shifted positions to improve the readability.

are assigned to the neutral components. Their IR spectra are represented by simple superimposition of the neutral constituent molecules.

The C_{60} complex includes benzene molecules for complex formation (1 : 2 : 1). The UV–Vis and IR spectra and high resistivity are consistent with its neutral nature. Its lattice parameters were reported previously.[36]

It is noticeable that the TENF molecules, the $E^1_{1/2}$ value of which (−0.14 V *vs.* SCE) is comparable or high compared with those of 2,5-QCl_2 (−0.15) and Cl_2NNQ (−0.20), affords a TDAP complex of neutral ground state while the latter two quinones give complexes with mixed ionicity.

6 Requirement for partial CT for TDAP complex

Fig. 11 shows the ionicity diagram of a CT complex between an electron donor (on the abscissa) and acceptor (on the ordinate). For the 1 : 1 CT complexes of the TTF·TCNQ system,[1b] it has been observed that the upper left region [$E^1_{1/2}(A) > E^1_{1/2}(D) + 0.02$; eqn. (1)] includes the strong CT complex with an ionic ground state. While the lower right region is for the weak complex. Just in between them a partial CT state ($1 > \gamma \geqslant 0.5$) with a segregated stack occurs [$E^1_{1/2}(D) + 0.02 \geqslant E^1_{1/2}(A) \geqslant E^1_{1/2}(D) - 0.34$; eqn. (2)].

A plot of the results of the TDAP ($E^1_{1/2}(D) = +0.02$) complexes clearly shows three regions: (**1**) ionic region where CT complex of D^{+2} is stable (indicated by closed circle), (**2**) partial CT region where $D^{+2(1-\delta)}$, $D^{+(2-2\delta+\gamma)}$, (D^{+2}, D^0) or (D^{+2}, A^{-1}, A^0) is created in the complex (open circle), and (**3**) neutral region where CT complex of D^0 and A^0 is generated (cross). Though we use different kinds of acceptor, namely TCNQs, quinones and others, the boundary between **1** and **2** is very clearly expressed by eqn. (9), which is represented by an upper solid line in Fig. 11.

$$\Delta E(DA) = -0.15 \text{ V } \textit{vs.} \text{ SCE} \quad (9)$$

The boundary defined by eqn. (9) is shifted by about 0.13 V into a much stronger acceptor side compared with that defined by eqn. (1). It is of interest that the TCNQ molecule ($E^1_{1/2} = 0.22$ V) resides in the region **1** with close proximity to the boundary of eqn. (9). Thus, it is expected that the C_{10}TCNQ or MeTCNQ molecules, which locate near the boundary of eqn. (9), may also afford a 1 : 4 partial CT complex.

The lower boundary between regions **2** and **3**, however, is not clear in Fig. 11 owing to the unsuccessful formation of solid CT complexes with acceptors weaker than 2,3-dichloro-5-nitro-1,4-naphthoquinone (Cl_2NNQ) and stronger than 2,4,7-trinitrofluoren-9-one (TNF). Probably the boundary lies very close to the complexes of 2,5-QCl_2, Cl_2NNQ and TENF since the first two afford mixed CT complexes and the last forms a neutral complex; $\Delta E(DA) \approx 0.19$ V *vs.* SCE, *i.e.*, the lower solid line in Fig. 11.

At present the region **2** is determined by eqn. (10), with one exception: the DTNF complex. The redox width for a partial CT state given by eqn. (10) 0.34 V, is nearly equal to that given by eqn. (2), 0.36 V.

$$-0.15 < \Delta E(DA) < -0.15 \text{ V } \textit{vs.} \text{ SCE} \quad (10)$$

It is expected that in the upper left side of Fig. 11 other regions appear which include very ionized species such as $D^{+3(1-\delta)}$ and/or $D^{+4(1-\delta)}$ ($\delta \geqslant 0$) by a combination with very strong acceptors.[13] With very weak acceptor C_{60}, it was clearly pointed out that TDAP is not strong enough by at least about 0.25 V to give rise to even a partial charge on the C_{60} molecules.

7 Summary

The TDAP molecule is a much stronger electron donor compared to conventional donor molecules such as TMTTF, *N*,*N*,*N*′,*N*′-tetramethyl-*p*-phenylenediamine and *N*,*N*-dimethyldihydrophenazine. Both the first and second redox processes involve consecutive two-electron transfer and the difference between these potentials is remarkably small indicating that the TDAP molecule easily releases four electrons. The molecular structure of TDAP reveals a rather flat molecular plane from which only one methyl group of each dimethylamino group deviates. The molecular orbital calculation and molecular structure of TDAP are not consistent with the ease of simultaneous two-electron release. The optimized structures of the neutral and charged species of TDAP ($+1 \sim +4$) suggest that the distortion of the benzene rings attached by two dimethylamino groups in the TDAP molecule is a critical factor for the ease of the release of four electrons in two steps. Solid complex formation with a variety of TCNQs, *p*-benzoquinones and other acceptors was examined. The ionicity of the ground state of the complexes was examined by UV–Vis–NIR and IR spectra, stoichiometry, conductivity and magnetic measurements. No solid CT complexes consisting of D^{+1} were prepared. F_4TCNQ gives a 1 : 1 complex of ($TDAP^{+2}$)(F_4TCNQ^{-2}). Other complexes of TCNQs contain D^{+2}, $D^{+2(1-\delta)}$ or $D^{+(2-2\delta+\gamma)}$ (δ, $\gamma \sim 0$) species except the 1 : 4 TCNQ complex, the donor part of which is deduced to be a mixture of D^{+2} and protonated TDAP, H_nD^{+n}. The partially ionic CT complexes of TCNQs are highly conductive and exhibit optical absorption bands below 5×10^3 cm^{-1}. The ionicity diagram of the 1 : 1–1 : 3 TDAP complexes was constructed and the criterion to afford partial CT state of the TDAP complexes including $D^{+2(1-\delta)}$, $D^{+(2-2\delta+\gamma)}$, ($D^{+2}+D^0$) or ($D^{+2}+A^{-1}+A^0$) species was obtained as $-0.15 < \Delta E(DA) < 0.19$ V *vs.* SCE, which is moved by +(0.13–0.15) V from that obtained for the TTF·TCNQ family.

Acknowledgements

This work was in part supported by a Grant-in-Aid for Scientific Research from the Ministry of Education, Science, Sports, and Culture, Japan, a Grant for CREST (Core Research for Evolutional Science and Technology) of Japan Science and Technology Corporation (JST), a fund for "Research for Future" from Japan Society for Promotion of Science and a fund for the International Joint Research Grant Program of the New Energy and Industrial Technology Development Organization (NEDO).

References

1 J. B. Torrance, *Acc. Chem. Res.*, 1979, **12**, 79; G. Saito and J. P. Ferraris, *Bull. Chem. Soc. Jpn.*, 1980, **53**, 2141; D. O. Cowan, in *Proceedings 4th International Kyoto Conference on New Aspects of Organic Chemistry*, eds. Z. Yoshida, T. Shiba and Y. Oshiro, Prentice-Hall, Englewood Cliffs, NJ, 1992.

2 L. F. Mott, *Metal-Insulator Transitions*, Taylor & Francis Ltd., London, 1974; C. S. Jacobsen, H. J. Pedersen, K. Mortensen and K. Bechgaard, *J. Phys. C: Solid State Phys.*, 1980, **13**, 3411; S. D. Obertelli, R. H. Friend, D. R. Talham, M. Kurmoo and P. Day, *J. Phys.: Condens. Matter*, 1989, **1**, 5671; U. Geiser, H. H. Wang, K. D. Carlson, J. M. Williams, H. A. Charlier Jr., J. E. Heindl, G. A. Yaconi, B. H. Love, M. W. Lathrop, J. E. Schirber, D. L. Overmyer, J. Ren and M.-H. Whangbo, *Inorg. Chem.*, 1991, **30**, 2586; T. Komatsu, N. Matsukawa, T. Inoue and G. Saito, *J. Phys. Soc. Jpn.*, 1996, **65**, 1340.

3 C. J. Gomez-Garcia, C. Gimenez-Saiz, S. Triki, E. Coronado, P. L. Magueres, L. Ouahab, L. Ducasse, C. Sourisseau and P. Delhaes, *Inorg. Chem.*, 1995, **34**, 4139; T. Nakamura, W. Minagawa, R. Kinami and T. Takahashi, *J. Phys. Soc. Jpn.*, 2000, **69**, 504; H. Seo, *J. Phys. Soc. Jpn.*, 2000, **69**, 805.

4 S. S. Pac and G. Saito, *Synth. Met.*, 1999, **102**, 1705; G. Saito, S. S. Pac , O. O. Drozdova, *Synth. Met.*, in the press.

5 A. F. Hebard, M. J. Rosseinsky, R. C. Haddon, D. W. Murphy, S. H. Glarum, T. T. M. Palstra, A. P. Ramirez and A. R. Kortan, *Nature*, 1991, **350**, 600.

6 Y. Misaki, H. Nishikawa, K. Kawakami, S. Koyanagi, T. Yamabe and M. Shiro, *Chem. Lett.*, 1992, 2321; T. Mori, H. Inokuchi, Y. Misaki, T. Yamabe, H. Mori and S. Tanaka, *Bull. Chem. Soc. Jpn.*, 1994, **67**, 661.

7 K. Takimiya, A. Ohnishi, Y. Aso, T. Otsubo, F. Ogura, K. Kawabata, K. Tanaka and M. Mizutani, *Bull. Chem. Soc. Jpn.*, 1994, **67**, 766.

8 J. P. Lu, *Phys. Rev. B Condens. Matter*, 1994, **49**, 5687; O. Gunnarsson, E. Koch and R. M. Martin, *Phys. Rev. B Condens. Matter*, 1996, **54**, R11026.

9 J. B. Torrance, J. J. Mayerle, K. Bechgaard, B. D. Silverman and Y. Tomkiewicz, *Phys. Rev. B Condens. Matter*, 1980, **22**, 4960; J. B. Torrance, Y. Tomkiewicz, R. Bozio, C. Pecile, C. R. Wolfe and K. Bechgaard, *Phys. Rev. B Condens. Matter*, 1982, **26**, 2267; H. Okamoto, Y. Tokura and T. Koda, *Phys. Rev. B*, 1987, **36**, 3858.

10 J. S. Miller, A. J. Epstein and W. M. Reiff, *Chem. Rev.*, 1988, **88**, 201; P.-M. Allemand, K. C. Knemani, A. Koch, F. Wudl, K. Holczer, S. Donovan, G. Grüner and J. D. Thompson, *Science*, 1991, **253**, 301.

11 J. W. Bray, H. R. Hart Jr., L. V. Interrante, I. S. Jacobs, J. S. Kasper, G. D. Watkins, S. H. Wei and J. C. Bonner, *Phys. Rev. Lett.*, 1975, **35**, 744; J.-L. Goudard, A. A. Lakhani and N. K. Hota, *Solid State Commun.*, 1982, **41**, 423.

12 N. Wiberg, *Angew. Chem.*, 1968, **80**, 809; T. Barth, C. Krieger, F. A. Neugebauer and H. A. Staab, *Angew. Chem., Int. Ed. Engl.*, 1991, **30**, 1028; T. Barth, C. Kriger, H. A. Staab and F. A. Neugebauer, *J. Chem. Soc., Chem. Commun.*, 1993, 1129; Y. Yamashita and M. Tomura, *J. Mater. Chem.*, 1998, **8**, 1933.

13 N. Ueda, Y. Sakata and S. Misumi, *Bull. Chem. Soc. Jpn.*, 1986, **59**, 3289. They described formation of a solid complex by the reaction between TDAP and I_2 in benzene. The stoichiometry was reported as $(TDAP)(I_2)_{4.4}$ by the elemental analysis of C, H, N and I (calc. C; 18.93, H; 2.10, N; 3.84, I; 74.33; obs. C; 19.16, H; 2.01, N; 3.73, I; 74.66%. However, the complex is more appropriately formulated as $(TDAP^{+3})(I_3^{-1})_3H_2O$ (calc. C; 18.78, H; 2.10; N; 3.65, I; 74.42%).

14 TDAP, IR: 2978, 2942, 2862, 2825, 2779, 1597, 1568, 1478, 1454, 1377, 1327, 1288, 1181, 1148, 1075, 940, 835 cm^{-1}, $TDAP(HCl)_4(H_2O)_x$ ($x=1$–2), IR: 3010, 2927, 2683, 1618, 1466, 1427, 1412, 1157, 1048, 980, 883, 829 cm^{-1}.

15 A. Altomare, G. Cascarano, C. Giacovazzo, A. Guagliardi, M. C. Burla, G. Polidori and M. Camalli, M. SIR92, adapted by S. Mackay for Crystan-GM, MAC Science Co. Ltd., 1995.

16 A. Kini, M. Mays and D. Cowan, *J. Chem. Soc., Chem. Commun.*, 1985, 286.

17 A. M.Kini, D. O. Cowan, F. Gerson and R. Mockel, *J. Am. Chem. Soc.*, 1985, **107**, 556.

18 K. Elbl-Weiser, C. Krieger and H. S. Staab, *Angew. Chem., Int. Ed. Engl.*, 1986, **25**, 1023.

19 M. R. Bryce, T. Finn, A. S. Batsanov, R. Kataky, J. A. K. Howard and S. B. Lyubchik, *Eur. J. Org. Chem.*, 2000, 1199.

20 T. Senga, K. Kamoshida, L. A. Kushch, G. Saito, T. Inayoshi and I. Ono, *Mol. Cryst. Liq. Cryst.*, 1997, **296**, 97.

21 Y. Kai, F. Hama, N. Yasuoka and N. Kasai, *Acta Crystallogr. Sect. B Struct. Crystallogr. Cryst. Chem.*, 1978, **34**, 1263.

22 E. G. Cox, D. W. J. Cruickshank and J. A. S. Smith, *Proc. R. Soc. London, Ser. A*, 1958, **247**, 1.

23 A. Dixton, J. C. Calabrese and J. S. Miller, *J. Phys. Chem.*, 1989, **93**, 2284.

24 J. S. Miller, D. A. Dixon, J. C. Calabrese, C. Vazquez, P. J. Krusic, M. D. Ward, E. Wasserman and R. L. Harlow, *J. Am. Chem. Soc.*, 1990, **112**, 381.

25 T. Sugimoto, E. Murahashi, K. Ikeda, Z. Yoshida, H. Nakatsuji, J. Yamauchi, Y. Kai and N. Kasai, *Mater. Res. Soc. Symp. Proc.*, 1992, **247**, 417.

26 J. S. Miller and J. C. Calabrese, *J. Chem. Soc., Chem. Commun.*, 1988, 63.

27 J. B. Torrance, B. A. Scott and F. B. Kaufman, *Solid State Commun.*, 1975, **17**, 1369; C. S. Jacobsen, in *Semiconductors and Semimetals*, ed. E. Conwell, **Vol. 27**, ch. 5, 1988, Academic Press, San Diego.

28 R. Bozio, I. Zanon, A. Girlando and C. Pecile, *J. Chem. Soc., Faraday Trans. 2*, 1978, **74**, 235.

29 S. G. Clarkson, B. C. Lane and F. Basolo, *Inorg. Chem.*, 1972, **11**, 662.

30 J. S. Chappell, A. N. Bloch, W. A. Bryden, M. Maxfield, T. O. Poehler and D. O. Cowan, *J. Am. Chem. Soc.*, 1981, **103**, 2242, It should be noted, however, that the authors of this paper used both the b_{1u} and a_g modes of C≡N stretching in their analysis. If one uses only the b_{1u} modes of IR spectra, the linear relation between $\nu_{C\equiv N}$ and the degree of CT(γ) is not held above $\gamma=0.5$.

31 R. L. Carlin, *Magnetochemistry*, p. 75, p. 184, Springer-Verlag, Berlin, 1986.

32 L. R. Melby, R. J. Harder, W. R. Hertler, W. Mahler, R. E. Benson and W. E. Mochel, *J. Am. Chem. Soc.*, 1962, **84**, 3374; C. J. Fritchie and P. Arthur, *Acta Crystallogr., Sect. B Struct. Crystallogr. Cryst. Chem.*, 1966, **21**, 139; K. D. Cummings, D. B. Tanner and J. S. Miller, *Phys. Rev. B Condens. Matter*, 1981, **24**, 4142.

33 A. R. Siedle, G. A. Candela and T. F. Finnegan, *Inorg. Chim. Acta.*, 1979, **35**, 125.

34 G. J. Ashwell, S. C. Wallwork and P. J. Rizkallah, *Mol. Cryst. Liq. Cryst.*, 1983, **91**, 359 and references cited therein.

35 T. Akutagawa, G. Saito, M. Kusunoki and K. Sakaguchi, *Bull. Chem. Soc. Jpn.*, 1996, **69**, 2487.

36 A. Otsuka, G. Saito, S. Hirate, S. Pac, T. Ishida, A. A. Zakhidov and K. Yakushi, *Mater. Res. Soc. Symp. Proc.*, 1998, **488**, 495.